Targeted Disruption of the *S1P$_2$* Sphingosine 1-Phosphate Receptor Gene Leads to Diffuse Large B-Cell Lymphoma Formation

Giorgio Cattoretti,[1] Jonathan Mandelbaum,[1] Nancy Lee,[3] Alicia H. Chaves,[4] Ashley M. Mahler,[3] Amy Chadburn,[2] Riccardo Dalla-Favera,[1] Laura Pasqualucci,[1] and A. John MacLennan[3]

[1]Institute for Cancer Genetics and the Department of Pathology, Herbert Irving Comprehensive Cancer Center, Columbia University and [2]Department of Pathology and Laboratory Medicine, Weill Medical College of Cornell University, New York, New York; [3]Department of Molecular and Cellular Physiology, University of Cincinnati, Cincinnati, Ohio, and [4]Department of Neuroscience, University of Florida College of Medicine, Gainesville, Florida

Abstract

S1P$_2$ sphingosine 1-phosphate receptor signaling can regulate proliferation, survival, morphology, and migration in many cell types *in vitro*. Here, we report that *S1P$_2^{-/-}$* mice develop clonal B-cell lymphomas with age, such that approximately half of the animals display this neoplasm by 1.5 to 2 years of age. Histologic, immunophenotypic, and molecular analyses revealed a uniform tumor phenotype with features of germinal center (GC)–derived diffuse large B-cell lymphoma (DLBCL). Tumor formation was preceded by increases in GC B cells and CD69$^+$ T cells, as well as an increased formation of spontaneous GCs, suggesting that *S1P$_2$* loss may promote lymphomagenesis in part by disrupting GC B-cells homeostasis. With the sole exception of rare lung tumors, the effect of *S1P$_2$* gene disruption is remarkably restricted to DLBCL. In humans, 28 of 106 (26%) DLBCL samples were found to harbor multiple somatic mutations in the 5′ sequences of the *S1P$_2$* gene. Mutations displayed features resembling those generated by the IgV-associated somatic hypermutation mechanism, but were not detected at significant levels in normal GC B cells, indicating a tumor-associated aberrant function. Collectively, our data suggest that S1P$_2$ signaling may play a critical role in suppressing DLBCL formation *in vivo*. The high incidence of DLBCL in *S1P$_2^{-/-}$* mice, its onset at old age, and the relative lack of other neoplasms identify these mice as a novel, and potentially valuable, model for this highly prevalent and aggressive human malignancy. [Cancer Res 2009;69(22):8686–92]

Introduction

Sphingosine 1-phosphate (S1P) can potently regulate the proliferation, survival, migration, and morphology of many cell types *in vitro* (1, 2). *In vivo* data implicate S1P in the physiology of the cardiovascular, immune, reproductive, and nervous systems (1–3). S1P elicits most of its effects via one or more members of a family of G protein–coupled receptors currently called S1P$_1$-S1P$_5$ (1–5). The S1P$_2$ receptor (previously named AGR16, H218, Edg-5, and LP$_{B2}$) binds S1P with nanomolar affinity and is ubiquitously expressed throughout development and adulthood (1–4).

S1P$_2$ couples to G$_i$, G$_q$, and G$_{13}$, leading to signaling through multiple pathways involving extracellular signal-regulated kinase/mitogen-activated protein kinase, cyclic AMP, c-Jun, c-Fos, Ca^{2+}, Rho, and Rac (1–5). S1P$_2$-dependent signaling has also been shown to mediate S1P-induced proliferation, survival, morphology, and migration in a wide variety of cell types in culture (1, 5).

S1P$_2$ knockout studies indicate essential *in vivo* roles in neuronal excitability during development (6), auditory and vestibular maintenance (7–9), and vascular tone (10). The signaling pathways and the cellular effects of S1P$_2$ both raise the possibility of S1P$_2$ involvement in cancer. *In vitro* manipulation studies have specifically addressed this issue, revealing that S1P$_2$ activation can inhibit cancer cell migration, invasion, and metastasis (11–13). However, the widespread *in vivo* expression of S1P$_2$, and its many cell type–dependent actions revealed in culture, make it difficult to predict what *in vivo* roles it may play in cancer.

We report here that targeted disruption of the *S1P$_2$* gene in mice leads to a high incidence of lymphoma formation with aging. These tumors display a remarkably uniform diffuse large B-cell lymphoma (DLBCL) phenotype of germinal center (GC) origin preceded by an increase in GC B cells and spontaneous GC formation. Moreover, the *S1P$_2$* 5′ sequences were found to be mutated in 26% of human DLBCL, but not in normal GC B cells, suggesting that *S1P$_2$* is aberrantly targeted by somatic hypermutation (SHM) in this lymphoma (14). Overall, these data suggest that S1P$_2$ may play a nonredundant *in vivo* role in suppressing DLBCL formation.

Materials and Methods

S1P$_2$ knockout mice. The mouse *S1P$_2$* gene was targeted through homologous recombination as previously described, leading to the deletion of the complete protein-coding region of this gene (6). *S1P$_2^{-/-}$* mice and *S1P$_2^{+/+}$* controls were generated on a 50:50 129SvEvBrd/C57Bl/6 background via *S1P$_2^{+/-}$* intercrosses and were genotyped by Southern blot or PCR of tail DNA. An additional cohort was generated on a pure 129SvEvBrd background. *S1P$_2^{-/-}$* mice were born at the predicted Mendelian frequency (6). They were maintained under standard housing conditions and monitored for abnormalities up to 18 to 24 mo of age.

In our previous study, some *S1P$_2^{-/-}$* mice in the mixed genetic background were observed to have rare (mean, <4), brief (mean, <5 s) seizures during development and an ~15% overall death rate from the seizures (6). On a pure 129SvEvBrd background, the overall *S1P$_2^{-/-}$* death rate drops below 5%.[5]

All experimental data were collected and analyzed without prior knowledge of genotype. All mice were cared for in accordance with the University of Cincinnati and Columbia University Institutional Animal Care and Use Committees.

[5] A.J. MacLennan et al., unpublished data.

Note: Supplementary data for this article are available at Cancer Research Online (http://cancerres.aacrjournals.org/).

L. Pasqualucci and A.J. MacLennan contributed equally to this work.

Requests for reprints: A. John MacLennan, Department of Molecular and Cellular Physiology, University of Cincinnati, 231 Albert Sabin Way, Cincinnati, OH 45267-0576. Phone: 513-558-0667; Fax: 513-558-5738; E-mail: john.maclen@uc.edu or L. Pasqualucci, Institute for Cancer Genetics, Columbia University, 1130 St. Nicholas Avenue, New York, NY 10032. Phone: 212-851-5248; Fax: 212-851-5256; E-mail: lp171@columbia.edu.

doi:10.1158/0008-5472.CAN-09-1110

SRBC immunization. For analysis of T cell–dependent immune responses, age- and sex-matched mice were immunized i.p. with 0.5 mL of a 2% SRBC suspension in PBS (Cocalico Biologicals), and sacrificed 10 d later.

Flow cytometry. The following antibody combinations were used on single-cell suspensions from normal organs or tumors: A: B220, IgM, IgD, and Ig κ light chain; B: B220, CD23, CD21, and CD11b; C: IgM, CD43, CD5, and CD19; D: B220, CD138, IgM, IgD, and Ig κ light chain; E: B220, CD69, and CD80; F: B220, A44.1, IgM, and CD43; G: CD3, CD4, CD8, and Vβ8 TCR. The enumeration of GC cells was performed by four-color staining with B220, Peanut Agglutinin (PNA), CD38, and GL7. All antibodies were from BD Pharmingen, except for the IgD-Pe (Southern Biotechnology, Inc.). Data were acquired on a FACSCalibur (Becton Dickinson) and analyzed with the FlowJo software (Tree Star, Inc.).

For cell proliferation measurements, 2 mg BrdUrd (Roche Biochemical) was injected 2 h before sacrifice. Four-color BrdUrd staining (Pharmingen) was performed on surface-labeled cells according to the manufacturer's instructions. Membrane exposure of phosphatidylserine in apoptotic cells was measured with recombinant, phycoerythryn-labeled AnnexinV (Pharmingen), and 7-AminoActinomycin D (Sigma) staining identified dead cells.

Histology, immunohistochemistry, and immunofluorescence. Four-micrometer-thick formalin-fixed, paraffin-embedded sections were stained for H&E or immunostained as published previously (15) using the following primary antibodies: rabbit anti-BCL6 (N3), goat anti-IRF4 (sc-6059), goat anti-Pax5, goat anti-CD21 (sc-7028; Santa Cruz Biotechnology), donkey anti-IgM (Jackson Immunoresearch Laboratories), rat anti-B220, CD138 (BD Pharmingen), and PNA lectin (Vector). Double immunohistochemical stainings were performed as published previously (16) with noncrossreacting combinations of primary and secondary antibodies.

Morphometric quantitation of GCs was performed with ImageJ (RSB, NIH). Grayscale or color images were acquired at room temperature using a Nikon E600 microscope (Nikon USA), fitted with Planachromat 4×/0.10/30.0, 10×/0.25/10.5, 20×/0.40/1.3, PlanApo 40×/0.095/0.12 to 0.16 (light microscopy) objectives, with a SPOT-2 CCD camera and software (Diagnostic Instruments). All images were edited for optimal color contrast with Adobe Photoshop 7 whole-image autocontrast feature, cropped, then mounted and labeled with Adobe Illustrator 10 (Adobe Systems), on an Apple G4 computer (Apple Computers).

Southern blot analysis and SHM analysis of Ig genes. Genomic DNA was isolated from tumor specimens by the salting out method, and screened for the presence of clonal immunglobulin heavy chain (IgH) gene rearrangements by Southern blot analysis according to standard procedures. Briefly, 5 μg of DNA were digested with EcoRI, separated by electrophoresis through a 0.8% agarose gel, transferred to nylon membranes, and hybridized with a radiolabeled fragment specific for the murine JH4 region.

For mutational analysis, the rearranged Ig variable heavy chain genes were amplified from genomic DNA as described (17); in a subset of samples, cDNA synthesis and reverse transcription-PCR (RT-PCR) amplification were also performed using primers specific for all the major murine IGVH families, and the protocols are available upon request. Amplicons indicative of clonal rearrangements (i.e., appearing as a discrete band on gel electrophoresis) were gel purified using the QIAQUICK purification method (QIAGEN) and sequenced directly to confirm the clonal nature of the rearrangement and to identify the presence of mutations. Since direct sequencing can only detect changes present in a significant fraction of the template DNA (i.e., clonally represented mutations), Taq errors are negligible and only mutations present in the clonal, tumor population are identified. Sequences were compared with the National Center for Biotechnology Information mouse genome databases and Ig sequence database, as well as to our own database to rule out polymorphisms or contamination with previously amplified rearrangements. All mutations were confirmed on independent PCR products.

RNA extraction and Northern blot analysis of S1P2 expression. Total RNA was extracted from 20 DLBCL cell lines using TRIZOL (Invitrogen), and Northern blot analysis was performed according to standard procedures, with radiolabeled probes corresponding to a fragment of the human *S1P2* cDNA, and glyceraldehyde-3-phosphate dehydrogenase (GAPDH) as a control for loading. The primers used for generation of the *S1P2* probe are S1P2RT-F1 (5′-tgccaaggtcaagctgtatg-3′) and S1P2RT-R1 (5′-agtccagaaggaggatgctg-3′). *S1P2* expression levels were then quantitated by Phosphorimager analysis and normalized with the GAPDH levels.

Results

S1P$_2^{-/-}$ mice develop lymphomas with aging. To examine the function of S1P$_2$ in tumorigenesis, a cohort of age-matched *S1P2*$^{-/-}$ and *S1P2*$^{+/+}$ mice was monitored for the occurrence of pathologic events over a period of 2 years. Complete necropsies, performed on eight *S1P2*$^{+/+}$ and nine *S1P2*$^{-/-}$ mice found dead between 14 and 23 months of age, revealed the presence of extensive lymphoma involvement in four of the *S1P2*$^{-/-}$ mice, whereas only one of the *S1P2*$^{+/+}$ mice had a pathologic mass on its spleen that could not be diagnosed due to severe tissue autolysis. Following these observations, we sacrificed and analyzed 13 randomly selected 19- to 24-month-old *S1P2*$^{-/-}$ mice and 11 age-matched *S1P2*$^{+/+}$ controls deriving from the same breeding pairs (in many cases, littermates). Complete necropsies of these mice revealed lymphomas in 7 of 13 (54%) of the *S1P2*$^{-/-}$ mice (total, 11 of 22) but none of the *S1P2*$^{+/+}$ controls (total, 1 possible of 19). Tumors were found in mesenteric, submandibular, and mediastinal lymph nodes; in the spleen; and rarely in liver and retroperitoneal soft tissue, with frequent involvement of multiple sites within individual animals. Tumors with the same characteristics were subsequently seen on a pure 129SvEvBrd background, with 6 of 9 (66%) of the 18- to 24-month-old *S1P2*$^{-/-}$ mice examined displaying lymphomas, in contrast to 0 of 9 of the age-matched *S1P2*$^{+/+}$ controls. Therefore, in total, 17 of 31 (54.8%) *S1P2*$^{-/-}$ mice were found affected compared with 1 possible of 28 (3.6%) *S1P2*$^{+/+}$ controls. In addition to the lymphoid malignancies, 3 of 31 (10%) *S1P2*$^{-/-}$ mice showed evidence of lung tumors, including two adenocarcinomas and one very large lung adenoma that could be classified as a carcinoma based on its size. No such abnormalities were present in the 28 *S1P2*$^{+/+}$ controls. With the exception of the comparatively low incidence of lung lesions, no other neoplasms were associated with *S1P2* gene disruption despite the high incidence of lymphomas. The few *S1P2*$^{+/-}$ mice that underwent full histopathologic analysis (data not shown) displayed neither lymphomas nor lung lesions, consistent with previous reports documenting the lack of other *S1P2*$^{-/-}$–associated phenotypes in heterozygous animals (e.g., refs. 6, 7).

S1P$_2^{-/-}$ lymphomas uniformly display the features of GC-derived DLBCLs. Histologic characterization of the lymphoma tissue from the *S1P2*$^{-/-}$ mice revealed infiltration by large atypical blast cells admixed with variable amounts of reactive inflammatory and lymphoid cells, consistent with the diagnosis of DLBCL, according to the Bethesda classification for murine lymphoid neoplasms (Fig. 1, *left*; ref. 18). Benign splenic marginal zone hyperplasia was diagnosed in three mice, two of which concomitantly displayed a nodal DLBCL. Immunohistochemical and flow cytometric analysis of the lymphomas indicated a GC origin (B220+, PNA+, BCL6+, Pax5+, IgMk dim/negative, IgD–, mostly CD5–, CD23–) without plasmacytic (CD138–, IRF4–) or monocytoid/marginal zone differentiation (CD21–, CD11b–, CD80–; data not shown; Figs. 1 and 2*A*). One of five tumors also displayed evidence of isotype switching (i.e., surface IgK positive, negative for preswitch isotypes IgD and IgM). RT-PCR analysis consistently documented expression of AID, the molecule required for SHM and class switch recombination in GC B cells (19), in all samples studied (Fig. 2*B*). The lymphomas did not express activation markers (CD69–, IRF4–).

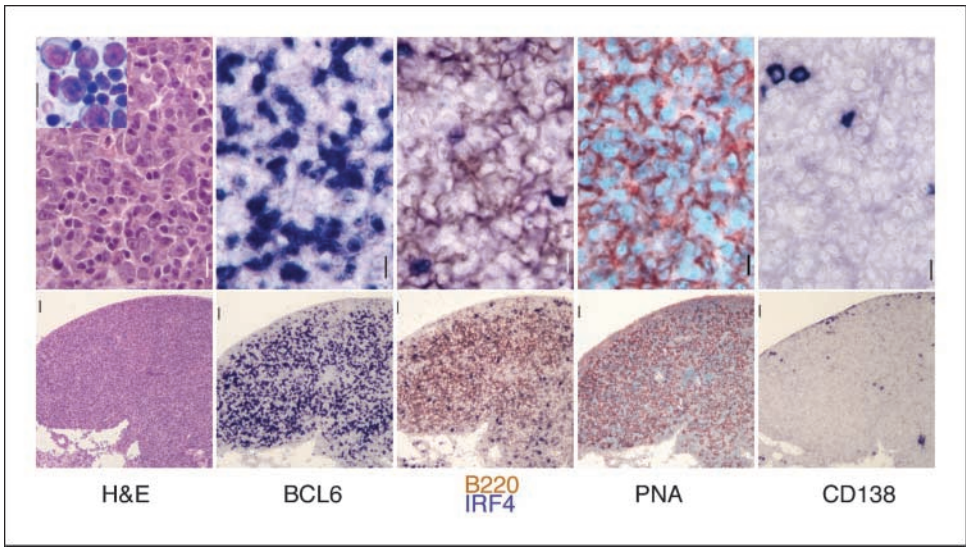

Figure 1. Histopathology of DLBCL in $S1P_2^{-/-}$ mice. Representative DLBCL, featuring H&E staining (note the large tumor cells in the Wright-Giemsa–stained touch preparation in the inset). These tumor cells display positive BCL6 (*dark blue*), B220 (*purple gray*), and PNA (*reddish brown*) staining, and negative IRF4 (*dark blue*) and CD138 (*dark blue*) staining. The lymph node is totally replaced by diffuse large cell lymphoma proliferation, containing lymphocytes and inflammatory cells (BCL6, B220, and PNA negative, and IRF4 and CD138 positive). The PNA-stained section also received a light blue nuclear counterstain. *Scale bars,* 10 μm (*bottom*) and 1 μm (*top*).

Southern blot analysis of the IgH locus by using a JH probe confirmed the clonal origin of the tumors in all samples studied (n = 4/4), as documented by the presence of distinct bands representing clonally rearranged Ig genes (Fig. 3*A*). In cases 297 and 246, the detection of two and three bands, respectively, may reflect the derivation from a clone where both Ig alleles had been rearranged, as it occurs in ~30% of B cells when the first rearrangement is not productive (20), or it may indicate a biclonal tumor, or both. The relative intensity of the residual germline band observed in all tumors is consistent with the presence of nonneoplastic cells in the biopsy, especially evident in the splenic tumors (case #240). Direct sequencing analysis of the rearranged IgV genes confirmed the clonal origin of the lymphomas and showed evidence of SHM in all samples analyzed (Fig. 3*B* and *C*). Overall, these data indicate that the DLBCL in $S1P_2^{-/-}$ mice derive from the clonal expansion of a cell that transited the GC.

$S1P_2$ gene disruption leads to alterations in the immune system before tumor formation. To test whether lymphoma development in $S1P_2^{-/-}$ mice is preceded by polyclonal abnormalities in B-cell differentiation and maturation, we performed an extensive characterization of the B-cell and T-cell compartments in young (7- to 8-week-old) and 9- to 12-month-old animals, by using flow

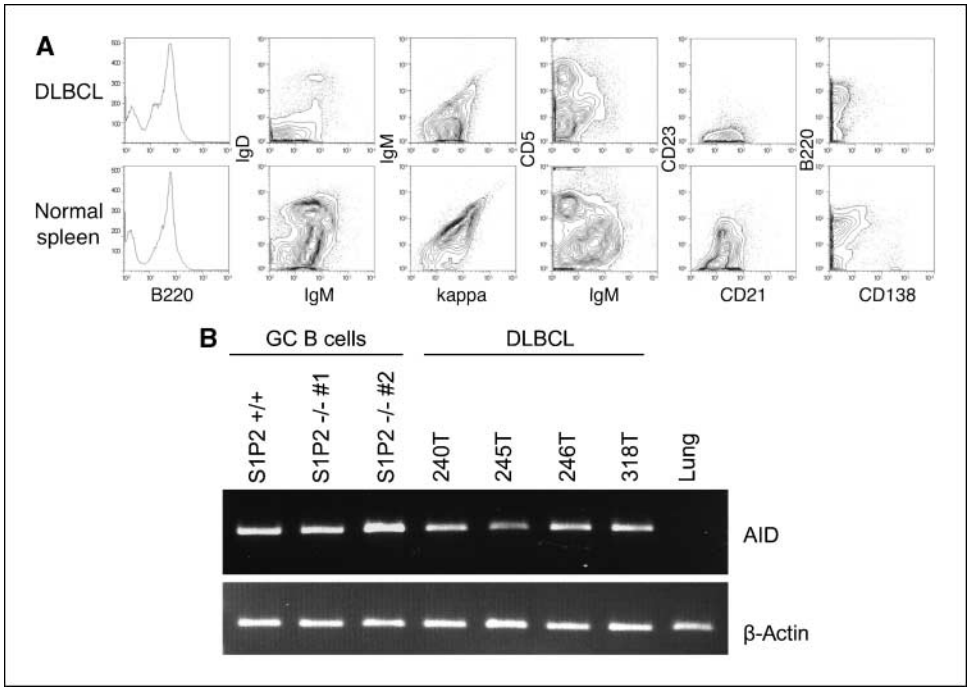

Figure 2. DLBCL immunophenotype in $S1P_2^{-/-}$ mice. *A,* surface immunophenotype by FCM of a representative DLBCL from a $S1P_2^{-/-}$ mouse and a histologically normal spleen from a littermate control $S1P_2^{+/+}$ mouse. Note the low/absent surface Ig, the loss of CD23, and the absence of CD138 in the DLBCL sample. *B,* AID expression in representative DLBCL from $S1P_2^{-/-}$ mice, compared with purified normal GC B cells from two $S1P_2^{-/-}$ and one $S1P_2^{+/+}$ mice. Mouse lung tissue was used as a negative control for the AID RT-PCR.

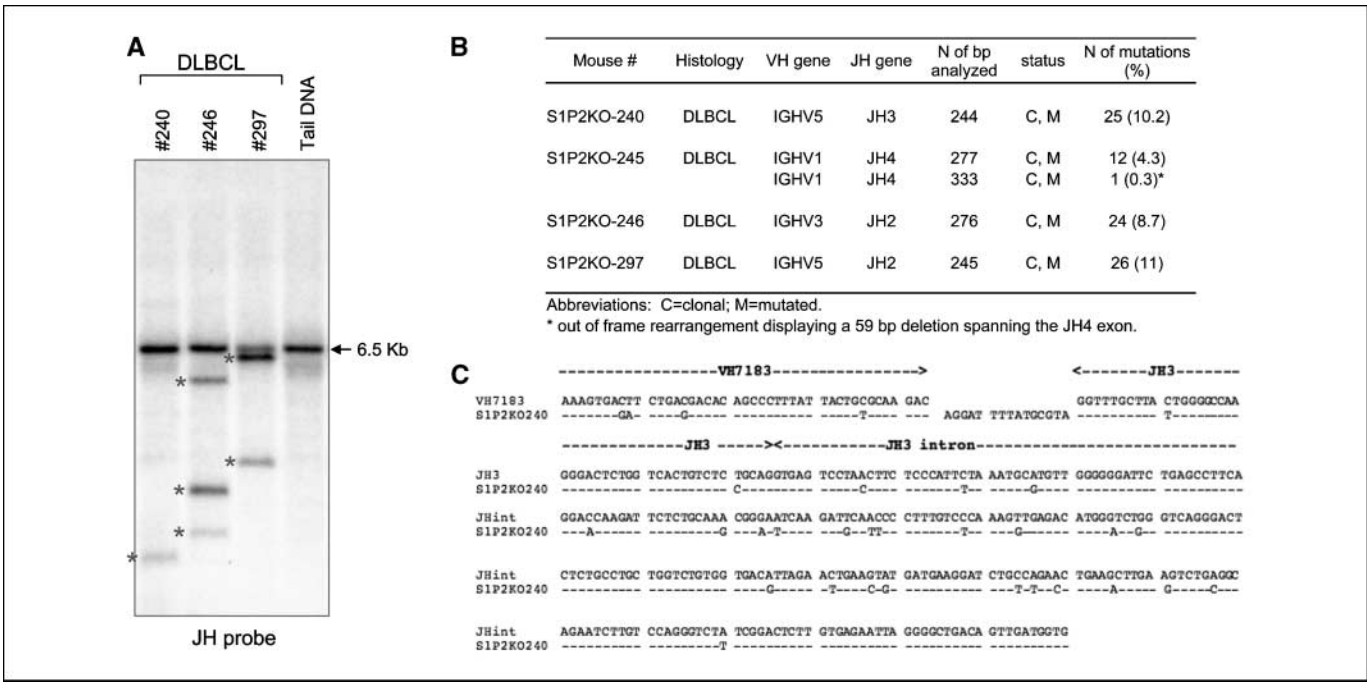

Figure 3. Clonal rearrangements of the IgH locus and evidence of SHM in DLBCL from *S1P$_2^{-/-}$* mice. *A,* Southern blot analysis of EcoRI-digested DNA from representative *S1P$_2^{-/-}$* DLBCLs, and control tail DNA, hybridized with a murine JH region probe. The germline immunoglobulin heavy chain EcoRI fragment is ~6.5 Kb (*arrow*). *, clonal rearrangements of the IgH gene in the tumors analyzed. The predominant germline band observed in some tumors is most likely due to the presence of infiltrating normal cells (see text). *B,* mutation analysis of clonally rearranged IgV genes in lymphomas from representative *S1P$_2^{-/-}$* animals. Note that although Southern blot analysis in tumors #246 and #297 suggests the presence of two distinct clones, only one rearranged allele could be successfully amplified, possibly due to the usage of a less common V gene family member not recognized by the primers used, or to the presence of mutations in the primer binding site. *C,* nucleotide sequence alignment of the rearranged IgV gene from *S1P$_2^{-/-}$* DLBCL #245 (as obtained by direct sequencing) with the germline VH7183 and JH region. *Dashes,* sequence identities; the indicated nucleotides correspond to mutations. Note that since direct sequencing only detects clonally represented events, the observed mutations can be unequivocally attributed to the malignant clone.

cytometric and immunohistochemical analysis. Mature, immature, apoptotic, and necrotic T- and B-cell subsets were examined in bone marrow, spleen, thymus, peritoneal cavity, and peripheral blood. These experiments showed no significant abnormalities at the relatively early age of 7 to 8 weeks, except for a small increase in CD4+ T cells and a marginal, statistically insignificant increase in CD23–/CD21– B cells (Supplementary Fig. S1). In contrast, flow cytometry analysis of nonimmunized, 9- to 12-month-old animals revealed an increase in the number of B220+PNA+ GC B cells in *S1P$_2^{-/-}$* mice (Fig. 4*A, inset*), compared with their littermate *S1P$_2^{+/-}$* and *S1P$_2^{+/+}$* controls. Immunohistochemical and morphometric analysis of GC formation in spleen tissue from the same animals confirmed that the *S1P$_2^{-/-}$* spleens contain an increase in both number and size of spontaneous GCs (Supplementary Fig. S2; Fig. 4*A* and *B*), in the absence of overt tumor formation. Given the BCL6+, PNA+ GC phenotype of the DLBCL that develop later in life, these data support the possibility that *S1P$_2$* gene disruption leads to DLBCL by altering GC B-cell regulation. These differences were not detected when the animals were analyzed after immunization with SRBC as a potent stimulus to evaluate T cell–dependent GC responses (Fig. 4*C*), possibly because the maximal response evoked by strong antigen delivery masked the effects of chronic low level GC stimulation.

S1P$_2^{-/-}$ mice were indistinguishable from the wild-type controls with respect to apoptosis (measured by AnnexinV binding and 7-AminoActinomycin D uptake) and proliferation (measured by BrdUrd incorporation) of GC cells (data not shown), as well as spleen size (absolute weight or relative to body weight), spleen follicle immunoarchitecture, *in situ* distribution of marginal zone B cells, defined by CD21 staining (Supplementary Fig. S3), and other B-cell subpopulations including CD69+ B cells (data not shown; Supplementary Fig. S4*A*). Therefore, the immunologic defects resulting from *S1P$_2$* gene disruption are clearly distinct from the marginal zone B-cell abnormalities recently reported for *S1P$_3^{-/-}$* mice (21).

In the T-cell compartment, analysis of 9- to 12-month-old mice revealed a significant increase in both the percentage (*S1P$_2^{-/-}$*, 14.9%; *S1P$_2^{+/+}$*, 8.0%; $P < 0.025$) and intensity of CD69-labeled cells (Supplementary Fig. S4*C*). CD69 is an activation-associated molecule that has a pleotropic immunoregulatory role (22) including fine tuning of the inflammatory and tumor-suppressor response through transforming growth factor β. It remains to be established whether the increase in CD69 expression results from retention of CD69+ cells or increased activation of T cells. No significant differences were observed in other parameters relative to T cell subsets from the spleen, thymus, lymph nodes and peripheral blood, including the percentage of Vβ8 TCR+ cells (Supplementary Fig. S4*B*).

The S1P$_2$ 5′ sequences are targeted by multiple somatic mutations in human DLBCL. To determine whether the *S1P$_2$* gene is altered in human DLBCL, we used PCR amplification and direct sequencing to analyze 106 samples (20 cell lines and 86 primary biopsies) for mutations in *S1P$_2$* 5′ sequences, and 20 samples (10 cell lines and 10 primary biopsies) for mutations in the *S1P$_2$* single protein-coding exon. Missense mutations of this exon were found in 2 of 20 cases (10%), including one cell line and one primary biopsy (Supplementary Table S1). In addition, 28 of 106 (26%) DLBCL samples carried one or more mutations distributed within the first ~1.3 Kb from the transcription start site, i.e., the hypermutable region in IgV and BCL6 genes (Table 1; Fig. 5; refs. 23–25). In total,

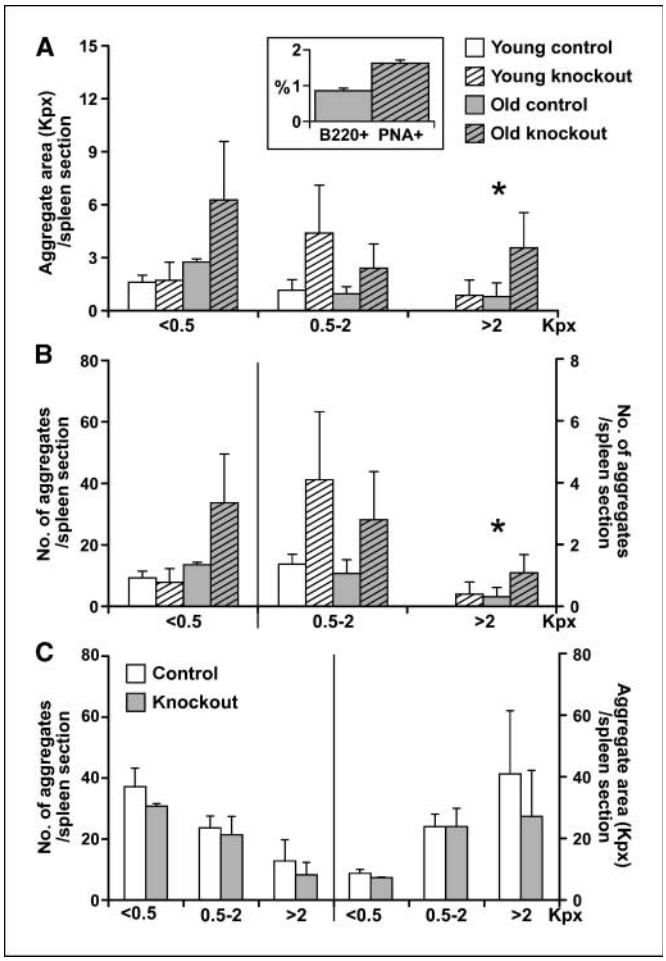

Figure 4. Morphometric analysis of splenic GC formation in $S1P_2^{-/-}$ mice. *A,* unimmunized mice; total area of BCL6+ aggregates in each size range [measured in pixels (1,000 pixels = 1 Kpx)] normalized for spleen section area. *Inset,* percentage of splenic B220+ PNA+ GC cells in old, unimmunized control and knockout mice measured by flow cytometry. The difference is significant ($P < 0.0015$). *B,* unimmunized mice; number of BCL6+ aggregates per spleen section area, calculated as described in *A*. The numbers presented are per average spleen section. *, ANOVA analyses indicated that both the size and number of >2 Kpx aggregates are significantly ($P < 0.05$) increased in $S1P_2^{-/-}$ spleens. *C,* number and area of the GC aggregates in SRBC-immunized mice. Note the expected increase in larger aggregates for immunized control and knockout mice compared with values for unimmunized mice in *A* and *B*. $n = 7$ young control, 3 young $S1P_2^{-/-}$, 4 old control, 3 old $S1P_2^{-/-}$. *Columns,* mean; *bars,* SEM.

114 sequence variants were detected in the 28 mutated cases, with an average mutation frequency of 0.17×10^{-2}/bp (range, 1–24 events/case; Supplementary Table S2; Table 1). Mutations were somatic in origin, as confirmed by analysis of paired normal DNA in cases with available material, and consisted in the vast majority of cases of single bp substitutions ($n = 105$), with occasional deletions and duplications of short DNA stretches ($n = 6$ and 3, respectively; Supplementary Table S2; Table 1). Of the 105 single bp substitutions observed, 61 were transitions and 44 were transversions, with a transition/transversion ratio of 1.38 (expected, 0.5; $P < 0.0001$; χ^2 test) and a preference for G+C versus A+T substitutions (Table 1). Furthermore, although the relatively low number of events prevented the assessment of statistical significance, the frequency of mutations targeting G residues within an RGYW motif was considerably higher than expected (14% versus 3.4%). Taken together, these features strongly resemble those described for the IgV-associated SHM mechanism (26), suggesting that the same machinery targets the *S1P2* gene in a sizable fraction of DLBCLs. Notably, sequencing analysis of this same region in 150 clones obtained from purified tonsillar centroblasts did not show significant levels of mutations, when compared with control pre-GC naïve B cells ($n = 75$) and fibroblasts ($n = 82$), both of which are known to lack SHM activity (mutation frequencies in the three populations: 0.013%, 0.006%, 0.011%; P = not significant; Supplementary Table S3). Thus, SHM of *S1P2* does not seem to represent a measurable phenomenon during the physiologic GC reaction, suggesting that the high mutation load suffered by the $S1P_2$ 5′ sequences in DLBCL reflects a tumor-associated aberration (14).

Northern blot analysis in the 20 DLBCL cell lines revealed heterogeneous *S1P2* expression, ranging from undetectable levels to levels comparable with those of GC B cells or type I Burkitt lymphoma lines, representing transformed GC B cells (Supplementary Fig. S5). No correlation was observed between steady-state expression levels and the presence or absence of aberrant SHM, nor with the mutation load.

Discussion

The present data show that *S1P2* gene disruption in mice leads to tumor formation, indicating a role for this gene as a nonredundant tumor suppressor *in vivo*. Although a low percentage of the tumors observed were lung adenocarcinomas—warranting further studies with substantially larger groups of animals—the overwhelming majority of the tumors were mature B-cell lymphomas displaying histologic and molecular features of GC-derived DLBCL, suggesting that $S1P_2$ plays a particularly critical role in suppressing such lymphoma formation.

The mechanism by which loss of *S1P2* promotes DLBCL development remains to be elucidated. One of the main effects of *S1P2* deletion in this model is the expansion of the GC compartment, as documented by an increase in the number and size of spontaneous GCs before any anatomic indication of tumor formation. Moreover, the histologic, immunophenotypic, and molecular features of the lymphomas developing later in life indicate their derivation from a cell that has experienced the GC reaction. Taken together, these observations suggest that loss of *S1P2* promotes lymphomagenesis in part by disrupting GC B-cell homeostasis, which in turn may lead to the accumulation of target cells for transformation, as seen in the Bcl-2-Ig model of lymphoma (27).

Table 1. Mutational analysis of the S1P2 5′ sequences in DLBCL

	Total	Cell lines	Primary cases
n of cases mutated/tested (%)	28/106 (26%)	5/20 (25%)	23/86 (27%)
Mutation frequency*	0.17%	0.18%	0.17%
n of single bp substitutions	105	21	84
n of deletions+duplications	9	1	8
Transitions/transversions (ratio)	61/44 (1.38)	16/5 (3.2)	45/39 (1.15)
G+C/A+T mutations	81/24	17/4	64/20

*Calculated in the mutated cases only, considering two alleles/sample (1,200 bp × 2).

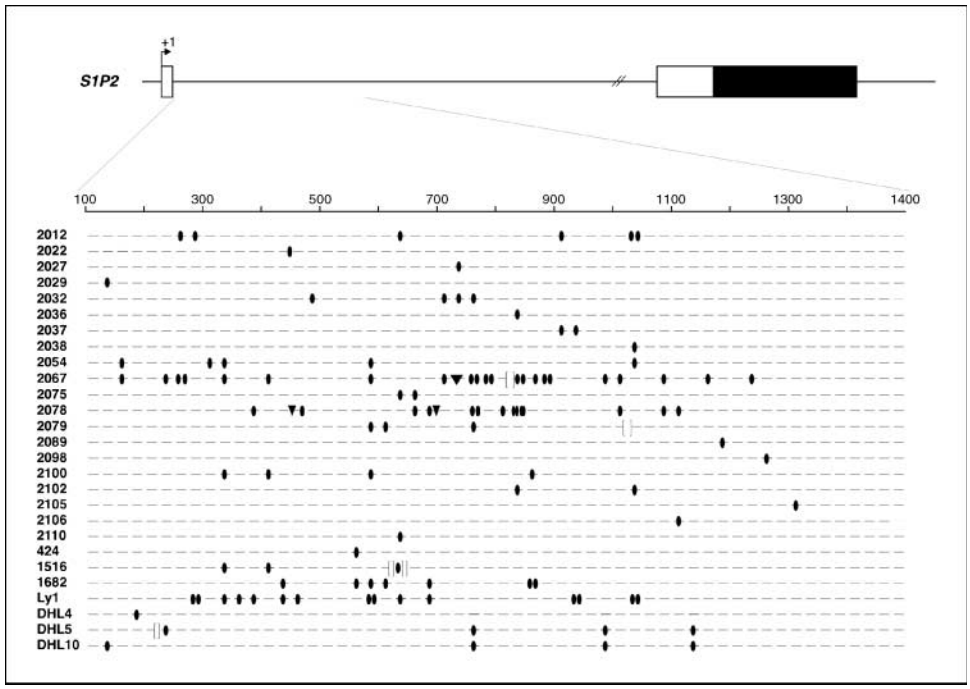

Figure 5. Mutational analysis of the *S1P$_2$* gene in human DLBCL. *Top, S1P$_2$* genomic locus with untranslated (*empty boxes*) and translated (*filled boxes*) exons; *arrow,* the transcriptional start site per GeneBank accession no. NM_004230. The region amplified for analysis is expanded in the bottom and aligned to sequences of mutated DLBCL cases (one line = two alleles), where each small segment represents a 25-bp interval and position +1 corresponds to the first nucleotide of the reference mRNA. *Ovals,* single basepair substitutions; *brackets,* deletions; *triangles,* insertions.

Future cell type–specific gene disruption studies will be required to definitively determine which cell types are involved in the S1P$_2$-dependent DLBCL suppression. One possibility is that the signaling involves S1P$_2$ receptors in GC B cells, given that: (*a*) purified normal GC centroblasts from mouse and human tonsils express *S1P$_2$* (Supplementary Fig. S6), consistent with the presence of *S1P$_2$* cDNA clones in an EST library constructed from purified GC B cells (NCI_CGAP_GCB1); (*b*) the S1P molecule is present in lymph and plasma at high enough concentrations to constitutively saturate such S1P$_2$ receptors (28); (*c*) S1P$_2$ receptors can regulate cellular differentiation, proliferation, survival, and migration in an apparently cell-autonomous manner, *in vitro* (1–5); and (*d*) the S1P$_2$ gene is aberrantly targeted by SHM in DLBCL cells, although the functional consequences of these mutations are still unknown (this study). Alternatively, S1P$_2$ receptors may regulate GC B-cell behavior, and DLBCL formation, by acting through other cell types involved in the GC reaction. These include dendritic cells, where expression of S1P$_2$ receptors may regulate their cytokine release (29), thereby indirectly influencing B cells. Furthermore, S1P$_2$ receptor expression has been detected in T cells (30, 31) and the subtle dysregulation of T-cell homeostasis in *S1P$_2^{-/-}$* mice may mediate enhanced GC precursor activation and increase the risk of lymphomagenesis. Notably, a recent report indicates that T cells can promote the production of large B-cell lymphomas, albeit with different characteristics than those of the *S1P$_2^{-/-}$* lymphomas (32).

Our study also identifies the *S1P$_2$* locus as a novel target of aberrant SHM in DLBCL. Mutations affecting putative *S1P$_2$* regulatory sequences were found in >25% of human DLBCL and were comparable in frequencies to other genes that are targeted by aberrant SHM in this disease, including PIM1, PAX5, RhoH/TTF, and MYC (Supplementary Fig. S7; ref. 14). Mutations also display the characteristic features of the IgV-associated SHM mechanism, but were not found at significant levels in purified normal GC B cells, indicating that they represent a tumor-specific phenomenon, presumably resulting from an aberrant function of the SHM machinery in DLBCL (14), and raising the possibility that some of these events may have been selected by the neoplastic clone for a role in deregulating S1P$_2$ expression. In the cell lines analyzed, the expression levels of *S1P$_2$* are variable, with some cases displaying very low to absent *S1P$_2$* mRNA. This scenario may in part reflect the known phenotypic and molecular heterogeneity of DLBCL (see the lack of significant *S1P$_2$* expression in both Ly3 and Ly10, which represents activated B-cell type DLBCL; ref. 33). However, *S1P$_2$* mRNA was also essentially absent in cell lines belonging to the GC B cell–derived subgroup, including the one (Ly1) that carries the highest number of mutations (Supplementary Fig. S5). Because S1P$_2$ is normally expressed in GC B cells, its absence in some DLBCL may represent a pathogenetic event. Given the extreme heterogeneity of the mutations, and their variable combination in individual cases, additional experiments will be required to determine the direct functional effect of each mutated allele on the regulation of S1P$_2$ expression and on DLBCL pathogenesis *in vivo*.

Notably, in a number of human DLBCL cases, the protein-coding sequence and presumed regulatory regions of the *S1P$_2$* gene are apparently intact. Therefore, although *S1P2* mutations may contribute to DLBCL in some cases (as discussed above), the intact S1P$_2$ receptors in the remaining cases raise the possibility that the receptor could serve as a potential therapeutic target in which S1P2 agonist treatment may decrease DLBCL formation by enhancing S1P2-dependent tumor suppression mechanisms. Clearly, the cellular and molecular aspects of the tumor suppression mechanisms need to first be elucidated.

The immunosuppressive drug FTY720 (FTY720-P) acts on S1P receptors to reduce T-cell and B-cell egress from lymphoid organs (31). Some data suggest it downregulates S1P$_2$ in addition to its effects on other S1P receptors (34). However, the *S1P$_2^{-/-}$* effects described here are likely unrelated given that: (*a*) the lymphocyte egress effects of FTY720 are mediated by the S1P1 receptor (31, 35); and (*b*) the *S1P$_2^{-/-}$* mice display neither the reduced blood lymphocyte populations (36, 37) nor the marginal zone B-cell displacement (35) seen with FTY720 administration.

The histology of the $S1P_2^{-/-}$ lymphomas, along with their expression of specific GC markers such as BCL6 and PNA, and the presence of IgV mutations, all strongly resemble the features of human DLBCL (38). In this respect, the $S1P_2^{-/-}$ tumors share significant properties with the tumors resulting from constitutive expression of BCL6 in B cells (16). In both models, GC-derived DLBCL develops with age following an increase in GC number, although the BCL6 mice display a modest splenomegaly and evidence of lymphoproliferative disease not seen with $S1P_2^{-/-}$ mice. *TCL1* overexpression in B and T cells and disruption of the *Bad* gene have also been reported to promote GC-derived DLBCL, although via different mechanisms that seem to be dependent on modification of B-cell proliferation and/or apoptosis (39, 40). Given the relatively higher incidence and the homogeneous phenotype of the $S1P_2^{-/-}$ lymphomas, this model may serve as a valuable new tool in the effort to determine the mechanisms regulating DLBCL formation.

Disclosure of Potential Conflicts of Interest

A.J. MacLennan holds a minority interest in $S1P_2$-related patents. The other authors declared no potential conflicts of interest.

Acknowledgments

Received 3/30/09; revised 7/28/09; accepted 9/8/09; published OnlineFirst 11/10/09.

Grant support: NIH grant CA37295 and a Leukemia & Lymphoma Society SCOR grant (R. Dalla-Favera).

The costs of publication of this article were defrayed in part by the payment of page charges. This article must therefore be hereby marked *advertisement* in accordance with 18 U.S.C. Section 1734 solely to indicate this fact.

We thank Danae Washton, Adina Grunn, and Glenn Doerman for excellent technical help, Lin Yang, Greg Boivin, the Molecular Pathology Facility of the Herbert Irving Cancer Center of Columbia University Medical Center, and the University of Cincinnati College of Medicine Pathology Core Facility for the superb histology service. L.P. is a Julie Gould Scholar.

References

1. Takabe K, Paugh SW, Milstien S, Spiegel S. "Inside-out" signaling of sphingosine-1-phosphate: therapeutic targets. Pharmacol Rev 2008;60:181–95.
2. Rivera R, Chun J. Biological effects of lysophospholipids. Rev Physiol Biochem Pharmacol 2006;160:25–46.
3. Choi JW, Lee C-W, Chun J. Biological roles of lysophospholipid receptors revealed by genetic null mice: an update. Biochim Biophys Acta 2008;1781:531–9.
4. Anliker B, Chun J. Cell surface receptors in lysophospholipid signaling. Cell Dev Biol 2004;15:457–65.
5. Toman RE, Spiegel S. Lysophospholipid receptors in the nervous system. Neurochem Res 2002;27:619–27.
6. MacLennan AJ, Carney PR, Zhu WJ, et al. An essential role for the H218/AGR16/Edg-5/LP(B2) sphingosine 1-phosphate receptor in neuronal excitability. Eur J Neurosci 2001;14:203–9.
7. MacLennan AJ, Benner SJ, Andringa A, et al. The S1P2-sphingosine 1-phosphate receptor is essential for auditory and vestibular function. Hear Res 2006; 220:38–48.
8. Herr DR, Grillet N, Schwander M, Rivera R, Muller U, Chun J. Sphingosine 1-phosphate (S1P) signaling is required for maintenance of hair cells mainly via activation of S1P2. J Neurosci 2007;27:1474–8.
9. Kono M, Belyantseva IA, Skoura A, et al. Deafness and stria vascularis defects in S1P2 receptor-null mice. J Biol Chem 2007;282:10690–6.
10. Lorenz JN, Arend LJ, Robitz R, Paul RJ, MacLennan AJ. Vascular dysfunction in S1P2 sphingosine 1-phosphate receptor knockout mice. Am J Physiol Regul Integr Comp Physiol 2007;292:R440–6.
11. Arikawa K, Takuwa N, Yamaguchi H, et al. Ligand-dependent inhibition of B16 melanoma cell migration and invasion via endogenous S1P2 G protein-coupled receptor. Requirement of inhibition of cellular RAC activity. J Biol Chem 2003;278:32841–51.
12. Yamaguchi H, Kitayama J, Takuwa N, et al. Sphingosine-1-phosphate receptor subtype-specific positive and negative regulation of Rac and haematogenous metastasis of melanoma cells. Biochem J 2003;374:715–22.
13. Lepley D, Paik JH, Hla T, Ferrer F. The G protein-coupled receptor S1P2 regulates Rho/Rho kinase pathway to inhibit tumor cell migration. Cancer Res 2005;65: 3788–95.
14. Pasqualucci L, Neumeister P, Goossens T, et al. Hypermutation of multiple proto-oncogenes in B-cell diffuse large cell lymphomas. Nature 2001;412:341–6.
15. Ye BH, Cattoretti G, Shen Q, et al. The BCL-6 proto-oncogene controls germinal-centre formation and Th2-type inflammation. Nat Genet 1997;16:161–70.
16. Cattoretti G, Pasqualucci L, Ballon G, et al. Deregulated BCL6 expression recapitulates the pathogenesis of human diffuse large B cell lymphomas in mice. Cancer Cell 2005;7:445–55.
17. Jolly CJ, Klix N, Neuberger MS. Rapid methods for the analysis of immunoglobulin gene hypermutation: application to transgenic and gene targeted mice. Nucleic Acids Res 1997;25:1913–9.
18. Morse HC III, Anver MR, Fredrickson TN, et al. Hematopathology subcommittee of the mouse models of human cancers consortium: Bethesda proposals for classification of lymphoid neoplasms in mice. Blood 2002;100:246–58.
19. Muramatsu M, Kinoshita K, Fagarasan S, Yamada S, Shinkai Y, Honjo T. Class switch recombination and hypermutation require activation-induced cytidine deaminase (AID), a potential RNA editing enzyme. Cell 2000; 102:553–63.
20. Yamada M, Wasserman R, Reichard BA, Shane S, Caton AJ, Rovera G. Preferential utilization of specific immunoglobulin heavy chain diversity and joining segments in adult human peripheral blood B lymphocytes. J Exp Med 1991;173:395–407.
21. Girkontaite I, Sakk V, Wagner M, et al. The sphingosine-1-phosphate (S1P) lysophospholipid receptor S1P3 regulates MAdCAM-1+ endothelial cells in splenic marginal sinus organization. J Exp Med 2004;200:1491–501.
22. Sancho D, Gomez M, Sanchez-Madrid F. CD69 is an immunoregulatory molecule induced following activation. Trends Immunol 2005;26:136–40.
23. Storb U, Peters A, Klotz E, et al. Somatic hypermutation of immunoglobulin genes is linked to transcription. Curr Top Microbiol Immunol 1998;229:11–9.
24. Shen HM, Peters A, Baron B, Zhu X, Storb U. Mutation of BCL-6 gene in normal B cells by the process of somatic hypermutation of Ig genes. Science 1998;280:1750–2.
25. Pasqualucci L, Migliazza A, Fracchiolla N, et al. BCL-6 mutations in normal germinal center B cells: evidence of somatic hypermutation acting outside Ig loci. Proc Natl Acad Sci U S A 1998;95:11816–21.
26. Neuberger MS, Ehrenstein MR, Klix N, et al. Monitoring and interpreting the intrinsic features of somatic hypermutation. Immunol Rev 1998;162:107–16.
27. McDonnell TJ, Korsmeyer SJ. Progression from lymphoid hyperplasia to high-grade malignant lymphoma in mice transgenic for the t(14; 18). Nature 1991;349:254–6.
28. Goetzl EJ, Wang W, McGiffert C, Huang M-C, Graler MH. Sphingosine 1-phosphate and its G protein-coupled receptors constitute a multifunctional immunoregulatory system. J Cell Biochem 2004;92:1104–14.
29. Idzko M, Panther E, Corinti S, et al. Sphingosine 1-phosphate induces chemotaxis of immature and modulates cytokine-release in mature human dendritic cells for emergence of Th2 immune responses. FASEB J 2002; 16:625–7.
30. Graeler M, Goetzl EJ. Activation-regulated expression and chemotactic function of sphingosine 1-phosphate receptors in mouse splenic T cells. FASEB J 2002;16: 1874–8.
31. Matloubian M, Lo CG, Cinamon G, et al. Lymphocyte egress from thymus and peripheral lymphoid organs is dependent on S1P receptor 1. Nature 2004;427: 355–60.
32. Zangani MM, Froyland M, Qiu GY, et al. Lymphomas can develop from B cells chronically helped by idiotype-specific T cells. J Exp Med 2007;204:1181–91.
33. Alizadeh AA, Eisen MB, Davis RE, et al. Distinct types of diffuse large B-cell lymphoma identified by gene expression profiling. Nature 2000;403:503–11.
34. Graler MH, Goetzl EJ. The immunosuppressant FTY720 down-regulates sphingosine 1-phosphate G-protein-coupled receptors. FASEB J 2004;18:551–3.
35. Cinamon G, Matloubian M, Lesneski MJ, et al. Sphingosine 1-phosphate receptor 1 promotes B cell localization in the splenic marginal zone. Nat Immunol 2004;5: 713–20.
36. Mandala S, Hajdu R, Bergstrom J, et al. Alteration of lymphocyte trafficking by sphingosine-1-phosphate receptor agonists. Science 2002;296:346–9.
37. Chiba K, Yanagawa Y, Masubuchi Y, et al. FTY720, a novel immunosuppressant, induces sequestration of circulating mature lymphocytes by acceleration of lymphocyte homing in rats. I. FTY720 selectively decreases the number of circulating mature lymphocytes by acceleration of lymphocyte homing. J Immunol 1998;160: 5037–44.
38. Küppers R, Klein U, Hansmann ML, Rajewsky K. Cellular origin of human B-cell lymphomas. N Engl J Med 1999;341:1520–9.
39. Hoyer KK, French SW, Turner DE, et al. Dysregulated TCL1 promotes multiple classes of mature B cell lymphoma. Proc Natl Acad Sci U S A 2002;99:14392–7.
40. Ranger AM, Zha J, Harada H, et al. Bad-deficient mice develop diffuse large B cell lymphoma. Proc Natl Acad Sci U S A 2003;100:9324–9.